



## Improving Bagasse Fly Ash Immobilized with *Spirulina* sp. as a Biosorbent for Fe<sup>3+</sup> Elimination from Wastewater in Physical Chemistry Laboratories

Sri Wahyuningsih<sup>1\*</sup>, Dyan Hatining Ayu Sudarni<sup>1</sup>, Ade Trisnawati<sup>1</sup>, Rima Nurjanah<sup>1</sup>

<sup>1</sup> Department of Chemical Engineering, Faculty of Engineering, Universitas PGRI Madiun

\*Email Correspondence: [swahyu@unipma.ac.id](mailto:swahyu@unipma.ac.id)

### Article history:

Submitted: 6 February 2026

Revision: 4 April 2026

Accepted: 11 May 2026

Online: 31 May 2026

DOI:

<http://doi.org/10.21111/atj.v10i1.22>

**ABSTRACT:** This work examined how to improve Bagasse Fly Ash (BFA) as an adsorbent by immobilizing it with *Spirulina* sp. biomass to remove Fe<sup>3+</sup> ions from effluent from physical chemistry laboratories. A common silica-rich agroindustrial by-product, BFA has a porous structure but little capacity for adsorption because there aren't many active functional groups. On the other hand, although *Spirulina* sp. has a lot of amino, hydroxyl, carboxyl, phosphate, and sulfate groups that allow for strong interactions with metal ions, its low mechanical stability and challenging post-treatment separation limit its direct application. *Spirulina* was immobilized in a sodium silicate matrix made from BFA using the sol-gel technique in order to get around these problems. This produced a composite that combined the chemical activity of the biomass with the structural benefits of BFA. FT-IR characterization revealed structural changes upon immobilization and verified the existence of functional groups in charge of metal binding. UV-Vis spectrophotometry at 510 nm was used to perform adsorption tests at contact periods of 15–60 minutes. In comparison to both *Spirulina* alone (44.920%) and unmodified BFA (37.038%), the immobilized BFA–*Spirulina* composite had the best Fe<sup>3+</sup> removal effectiveness (51.571% at 60 minutes). Synergistic interactions within the composite are responsible for this enhanced performance: *Spirulina* offers chemically active sites for complexation and electrostatic interactions with Fe<sup>3+</sup>, while BFA enhances physical adsorption and diffusion through its porous matrix. The outcomes show that the BFA–*Spirulina* composite is an efficient, affordable, and eco-friendly biosorbent that may be used to remediate laboratory waste that contains iron. By converting biological and agricultural wastes into valuable resources for environmental repair, this method also promotes waste valorization.

**Keywords:** adsorption; bagasse fly ash; biosorbent; Fe<sup>3+</sup>; immobilization; *Spirulina* sp.

### 1. INTRODUCTION

Chemistry laboratories frequently generate inorganic liquid waste, including waste that contains iron (III) ions or Fe<sup>3+</sup>. This waste comes from using compounds like

FeCl<sub>3</sub>, Fe(NO<sub>3</sub>)<sub>3</sub>, and Fe<sub>2</sub>(SO<sub>4</sub>)<sub>3</sub> in a variety of investigations, such as complex stability, redox reactions, and the assessment of the physicochemical properties of solutions. Fe<sup>3+</sup> ions are not considered a high-level

hazardous heavy metal, but they can nonetheless harm the environment if released untreated (Arita et al., 2022).

Fe<sup>3+</sup> waste management is now restricted to gathering trash in drums without any separation or pretreatment in many educational laboratories, including physical chemistry laboratories. Fe(OH)<sub>3</sub> precipitation, leakage, drum corrosion, and pH shifts owing to waste accumulation are some of the dangers linked with this temporary storage system. Inadequate management of Fe<sup>3+</sup> waste can lead to soil degradation, water turbidity, and the development of iron oxide deposits that are harmful to the surrounding environment and the laboratory environment (Ichsan et al., 2025).

However, the agroindustrial sector generates a lot of solid waste, including Bagasse Fly Ash (BFA) from burning sugarcane bagasse. BFA can be used as an adsorbent for heavy metals since it is cheap, plentiful, and rich in silica and amorphous carbon (Ahmad et al., 2018). However, BFA-only adsorption frequently has drawbacks, including a low adsorption capacity and challenges with post-adsorption separation. The creation of composite materials with enhanced stability and adsorption capacity is encouraged by this circumstance (Srivastava et al., 2006). Previous studies reported by (Patel, 2020) in the review article *Environmental Valorisation of Bagasse Fly Ash* stated that raw bagasse fly ash often exhibits relatively low adsorption performance due to its limited number of active sites and comparatively low specific surface area. Therefore, chemical activation and material modification are commonly applied to improve its adsorption efficiency.

In the meantime, functional groups including carboxyl, hydroxyl, phosphate, and amine found in the cell walls of the microalgae *Spirulina* sp. have a significant potential for biosorption of metal ions. Although *spirulina* has been demonstrated to interact with a variety of metal cations, including Fe<sup>3+</sup>, there are still obstacles to its

direct use, including its easily scattered biomass and the difficulty of extracting it after the adsorption process (Apriyani, 2018).

The immobilization approach is a desirable method for enhancing adsorption performance to get beyond these restrictions (Musnamar et al., 2025). Microalgae biomass can be combined with inert or porous materials through immobilization, producing a composite with improved surface area, stability, and ease of separation. A hybrid adsorbent material that combines the advantages of BFA as a porous material and *Spirulina* as an active biosorbent might be produced by combining the BFA–*Spirulina* immobilized composite (Mall et al., 2006). The idea of waste valorization—that is, using biological biomass and agroindustrial waste to solve laboratory waste issues supported by the synergy between the two, which is anticipated to boost the Fe<sup>3+</sup> adsorption capability. This study proposed a low-cost hybrid biosorbent combining BFA-derived silica matrix and *Spirulina* biomass for Fe<sup>3+</sup> adsorption from laboratory wastewater. This study proposes a low-cost hybrid biosorbent combining BFA-derived silica matrix and *Spirulina* biomass for Fe<sup>3+</sup> adsorption from laboratory wastewater.

## 2. MATERIALS AND METHODS

### 2.1 Tools and Material

A UV-Vis Spectrophotometer was the instrument utilized in this investigation. Bagasse Fly Ash (BFA) from the Redjosarie Magetan sugar mill, Commercial dried *Spirulina* algae was used as biosorbent biomass, Analytical grade NaOH, HCl, and Fe metal ion solution (FeCl<sub>3</sub>.6H<sub>2</sub>O) were the ingredients utilized. Using sodium thiosulfate to reduce Fe<sup>3+</sup> to Fe<sup>2+</sup> and then complexing it with 1,10-phenanthroline to generate an iron complex in the form of an orange solution, UV-Vis spectrophotometry was used to measure the iron content. EDTA, which serves as a masking agent to prevent other heavy metal ions from interfering with sample measurements, helped optimize the process. Furthermore, an acetate buffer solution with a pH of 4.5 was employed to

control and preserve the pH of the surrounding environment.

## 2.2 Maximum Wavelength Determination and Calibration Curve

Na<sub>2</sub>S<sub>2</sub>O<sub>3</sub> was used to decrease a standard Fe<sup>3+</sup> solution, which was subsequently reacted with 1,10-phenanthroline, EDTA, and acetate buffer at pH 4.5. After letting the mixture rest for 60 minutes, 5 mL of acetone were added and diluted to the appropriate level. Solutions with six concentration variations, ranging from 0 ppm to 5 ppm, were used to create a calibration curve. The procedures used were identical to those for figuring out the maximum wavelength (Leechart et al., 2016).

## 2.3 BFA Preparation

Bagasse fly ash is cleaned using distilled water and subsequently filtered heating for a full day at 100 °C in an oven. After that, a 100 mesh sieve is used to grind and filter the bagasse fly ash to a consistent size. Next, combine 40 grams of BFA with 400 mL of 0.1 M HCl. Heat while stirring for two hours. Whatman 41 filter paper was then used for filtering. Use a pH meter to verify that the pH is neutral before washing with hot distilled water. BFA is then dried for four hours at 105 °C (Kasman et al., 2022).

## 2.4. Producing Na Silicate

Mix 20 grams of BFA with 50 mL of 12M NaOH. At 80 °C, stir the mixture for four hours. Next, use Whatman No. 41 filter paper to filter the mixture. A solution of Na<sub>2</sub>SiO<sub>2</sub> was produced (Alnahhal et al., 2024).

## 2.5 Sample Preparation for Spirulina Algae

Use distilled water to clear the algae. Use a centrifuge and filter to separate the algae from the distilled water. For thirty days, let the cleansed algae dry at room temperature. The algae should next be ground and sieved through a 100-mesh screen to prepare it for immobilization (Moubayed & Al-Houri, 2022).

## 2.6 Algae Immobilization in Silica Gel

A 100 mL Na-silicate solution was taken, and concentrated HCl was added to it until it reached a neutral pH (pH=7). The mixture was then stirred to form an aqua-gel (hydrogel), and 3 grams of microalgae biomass was added. It was then dried in an oven at 80 °C (Zhang et al., 2025).

## 2.7 Adsorbent Characterization

The samples were dried at 80 °C for a full day before examination. KBr plates with 200 mg of phosphate and 1.5 mg of material were prepared for analysis. The IR wavenumber range (400-4000 cm<sup>-1</sup>) was then used to measure the spectra (Bhattacharjee et al., 2020).

## 2.8 Adsorption Experiments

Adsorption experiments were conducted by adding 0.100 g of adsorbent to 50 mL of Fe<sup>3+</sup> solution with an initial concentration of 125.235 mg/L. The solution pH was adjusted to 4.5 and agitated at 150 rpm at room temperature (27 ± 2 °C) for 15, 30, 45, and 60 min. After filtration, residual Fe concentration was measured by UV-Vis spectrophotometry at 510 nm using the 1,10-phenanthroline method. All experiments were performed in triplicate (n = 3). Data are presented as mean ± standard deviation and analyzed using one-way ANOVA followed by Tukey's post hoc test at level of significance p < 0,05 (Mohamed, 2025).

## 3. RESULTS AND DISCUSSION

### 3.1 Bagasse Fly Ash (BFA) Treatment

The Bagasse Fly Ash (BFA) waste utilized in this investigation was generated through the pyrolysis process of a combustion furnace operating at temperatures reaching 600 °C. The extreme heating process has resulted in the removal of the organic fraction of the bagasse, leaving predominantly the inorganic fraction, particularly SiO<sub>2</sub>. Bagasse fly ash (BFA) is industrial solid waste generated from burning of bagasse in steam boilers to generate electric energy in the sugar industry. In most developing countries, BFA is not commercialized and remains as a waste that

causes great problems for environmental disposal (Morentera et al., 2022). Studies have shown that it is a carbon- and silica-rich industrial waste which is cheap and available in large quantities in many sugar industries. It has been used as an adsorbent for removal of heavy metals, organic matter and dyes from water and wastewater under different treatment conditions. For instance, sugarcane bagasse powder is used as biosorbent for the removal of Reactive Red 120 (RR120) dye from aqueous solutions, achieving a maximum adsorption efficiency of 94.62% under optimum operating conditions. Lower pH levels, lower starting dye concentrations, and smaller particle sizes all improved the adsorption efficacy, suggesting that these factors have a major impact on the biosorption process (Ahmad et al., 2018).

The preparation of bagasse fly ash (BFA) was carried out to remove adhering impurities, homogenize particle size, and activate the surface before its use as an adsorbent. Initially, the raw BFA was washed thoroughly with distilled water to eliminate water-soluble impurities such as residual sugars, dust, and inorganic salts. The washed material was then dried in an oven at 100 °C for 24 h to remove physically adsorbed moisture, which could interfere with subsequent acid activation (Warna & Tekstil, 2016).

The dried BFA was ground and sieved through a 100-mesh sieve to obtain a uniform particle size, thereby minimizing mass transfer limitations and ensuring consistent adsorption behavior. A total of 40 g of sieved BFA was then treated with 400 mL of 0.1 M HCl under continuous stirring and heating for 2 h. This acid activation step serves several purposes: (i) dissolution of acid-soluble mineral impurities, (ii) removal of metal oxides that may block pores, and (iii) protonation of surface functional groups, which can increase the availability of adsorption sites (Subramanian et al., 2013).

After acid treatment, the suspension was filtered using Whatman No. 41 filter paper and washed repeatedly with hot distilled water until the filtrate reached neutral pH.

Achieving neutral pH is essential to ensure complete removal of residual hydrochloric acid, which could otherwise alter the solution pH during adsorption experiments and affect  $\text{Fe}^{3+}$  uptake. Finally, the activated BFA was dried at 105 °C for 4 h to remove residual moisture and obtain a stable adsorbent ready for further processing and characterization (Morentera et al., 2022).

Overall, this preparation procedure is expected to improve the adsorption performance of BFA by increasing surface cleanliness, enhancing pore accessibility, and exposing a greater number of active silanol and carbon-based functional groups involved in metal ion adsorption.

### 3.2 Spirulina as Biosorbent

In this investigation, The preparation of the algae biomass was carried out to remove residual impurities, reduce moisture content, and obtain a homogeneous powder suitable for immobilization. Initially, the algae were washed thoroughly with distilled water to eliminate adhering salts, dust, and other soluble contaminants that could interfere with the adsorption process or affect the interaction between the biomass and the silica matrix. Following the washing step, the algae suspension was separated from the washing medium by centrifugation and subsequent filtration. Centrifugation facilitated the efficient sedimentation of the algal cells, while filtration ensured complete removal of excess water. This step was essential to obtain clean and concentrated biomass prior to drying (Mohamed, 2025). The purified algae were then dried at room temperature for 30 days. Slow drying under ambient conditions helps preserve the structural integrity of the biomass and prevents thermal degradation of sensitive functional groups such as hydroxyl, amino, carboxyl, and sulfate groups, which play a significant role in metal ion adsorption.

After drying, the biomass was ground and passed through a 100-mesh sieve to produce a uniform particle size. Particle size homogenization increases the reproducibility of the immobilization process and improves

the accessibility of active adsorption sites by increasing the surface area. The resulting fine algae powder was then ready for immobilization within the silica matrix derived from bagasse fly ash.

The *Spirulina* biosorption features as well as that of other microalgal biomass been exploited for contaminants remediation in both soil and water environments. The capability of the *Spirulina* to adsorb contaminants from soil and wastewaters has rendered the biomass highly significant in environmental remediation. It possessed significant advantages because of its relative abundance, higher yield, and lower costs of production (Metwally et al., 2025). It is potential for elimination of heavy metals and organic pollutants from soil and wastewater. The *Spirulina* possess wider surface area to volume ratio, which sufficiently provides active sites for the adsorption of the contaminants. Moreover, the various functional groups in the *Spirulina* including the amino acids, hydroxyl groups and carboxyl groups create abundant adsorption sites for uptake and interaction with the contaminants via chemical and physical processes. The *Spirulina* served as low-cost option for physical and biological remediation compared to chemical methods. Several findings have been reported on the heavy metals removal from soil using the *Spirulina* (Collard & Blin, 2014). Also, reports are available in the literature for the treatment of smelter and refinery effluents, dyes, pharmaceuticals, and wide spectrum of organic contaminants, focusing more on industrial wastewater treatment or, more broadly, bioremediation of aquatic systems. Reports on removal of heavy metals and inorganic contaminants, from the wastewater is also available (Leechart et al., 2016). Its use in the soil and wastewater remediation contributes to environmental sustainability and serve as a valuable tool for addressing the persistent problem of the soils and waters contamination.

### 3.3 Synthesis of Sodium Silicate

The process of immobilizing microalgae with sodium silicate solution is carried out using the sol-gel method, which involves the addition of HCl. The addition of concentrated HCl solution aims to form free silicic acid, which can bind to form dimers, trimers, and so on through a polycondensation reaction and the release of H<sub>2</sub>O molecules. Sodium silicate was synthesized using the sol-gel method using a SiO<sub>2</sub> precursor extracted from BFA. Dissolving the ash in a 12 M NaOH solution produced a clear sodium silicate solution.

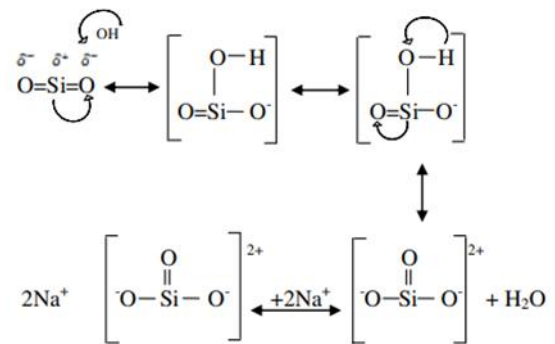


Figure 1. The reaction mechanism for the formation of sodium silicate (Alnahhal et al., 2024)

Figure 1. illustrates the chemical transformation of silica (SiO<sub>2</sub>) into sodium silicate through alkaline dissolution, followed by protonation to form silanol groups during the sol-gel process (Fouad et al., 2024).

Initially, hydroxide ions (OH<sup>-</sup>) attack the silicon atom in the Si-O-Si network of silica. This nucleophilic attack breaks one of the Si-O-Si bonds, generating a silicate species containing hydroxyl (Si-OH) and silanolate (Si-O<sup>-</sup>) groups. Through proton transfer and structural rearrangement, the silicate species is converted into a tetrahedral silicate anion.

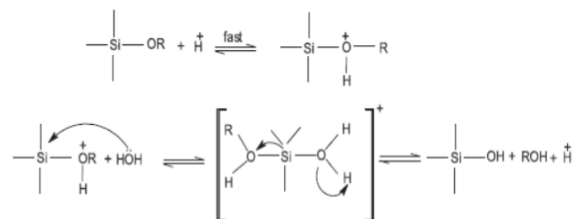
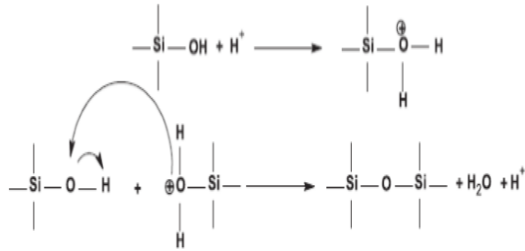


Figure 2. Hydrolysis reaction mechanism

In the presence of sodium ions ( $\text{Na}^+$ ), the negatively charged silicate species forms soluble sodium silicate ( $\text{Na}_2\text{SiO}_3$ ). This step explains the extraction of silica from bagasse fly ash using concentrated NaOH solution (Plana et al., 2025). When the sodium silicate solution is subsequently acidified, the sodium ions are displaced by protons ( $\text{H}^+$ ), producing silicic acid species containing silanol groups ( $\text{Si-OH}$ ).



**Figure 3.** Condensation reaction mechanism

In the presence of sodium ions ( $\text{Na}^+$ ), the negatively charged silicate species forms soluble sodium silicate ( $\text{Na}_2\text{SiO}_3$ ). This step explains the extraction of silica from bagasse fly ash using concentrated NaOH solution. When the sodium silicate solution is subsequently acidified, the sodium ions are displaced by protons ( $\text{H}^+$ ), producing silicic acid species containing silanol groups ( $\text{Si-OH}$ ). These silanol groups then undergo condensation reactions to form new  $\text{Si-O-Si}$  bonds, generating a three-dimensional silica gel network while releasing water as a by-product (Fouad et al., 2024).

Overall, the reaction sequence can be summarized as follows:

- a. Alkaline dissolution of silica (Fig. 1)  
 $\text{SiO}_2 + 2\text{NaOH} \rightarrow \text{Na}_2\text{SiO}_3 + \text{H}_2\text{O}$
- b. Acidification and hydrolysis (Fig. 2)  
 $\text{Na}_2\text{SiO}_3 + 2\text{H}^+ + \text{H}_2\text{O} \rightarrow \text{Si}(\text{OH})_4 + 2\text{Na}^+$
- c. Condensation (Fig.3)  
 $\text{Si}(\text{OH})_4 \rightarrow \text{SiO}_2 (\text{gel}) + 2\text{H}_2\text{O}$

This mechanism demonstrates how insoluble silica present in bagasse fly ash is converted into soluble sodium silicate and subsequently transformed into a silica matrix suitable for immobilizing *Spirulina*

biomass. In this investigation, a total of 100 ml of sodium silicate solution was added to 3 grams of algae powder while stirring with a stirrer until homogeneous. The mixture was slowly added with 1 M HCl drops until the pH reached 7. The gradual addition of 1 M HCl caused the solution to thicken (form a gel). Hydrochloric acid (HCl) was chosen as the catalyst and reactant in the sol-gel process because the pores it produces are more uniform than those of sulfuric and phosphoric acids. Furthermore, HCl is more effective, producing a higher silica content than  $\text{H}_2\text{SO}_4$ . The addition of hydrochloric acid to the precursor causes the protonation of the siloxy ( $\text{Si-O-}$ ) groups to form silanol ( $\text{Si-OH}$ ). With the help of an acid catalyst, siloxy groups ( $\text{Si-O-}$ ) then further attack the resultant silanol groups to create siloxane linkages ( $\text{Si-O-Si}$ ). This technique creates an amorphous silica network quickly and constantly. Acid-catalyzed condensation of a sol solution is comparable to the assault of  $\text{Si-O-}$  on  $\text{Si-OH}$  to generate  $\text{Si-O-Si}$ . A fully greenish-brown gel is formed by letting the mixture stand overnight. Since silica gel will form after 18 hours, this standing step is crucial. The resultant aqua gel is then dried for 12 hours at  $80^\circ\text{C}$  in an oven to create water-free silica algae. After being mashed using a mortar and pestle and sieved to a consistent size, the resulting silica algae adsorbent produces firm, smooth, brownish-white silica algae (Fathurohman et al., 2021). The optimal adsorption capacity is provided by a NaOH activating agent at a concentration of 12 M. The goal of this dissolving and subsequent melting is to guarantee that bagasse fly ash is fully converted to sodium silicate. After that, the mixture is heated to  $80^\circ\text{C}$  while being stirred with a stirrer for 4 hours to create a thick, black solution. The residue is then separated from the filtrate by filtering it through Whatman paper. The filtrate ( $\text{Na}_2\text{SiO}_3$  solution) produced is used as a precursor to produce silica-algae adsorbent.

### 3.4. Characterization of Spirulina and BFA-Silica Adsorbent

The primary determinant of adsorption efficacy is the properties of the adsorbent. Finding the active groups in each adsorbent that contribute to the adsorption process was the goal of the FT-IR study of Spirulina algae, both before and after immobilization.

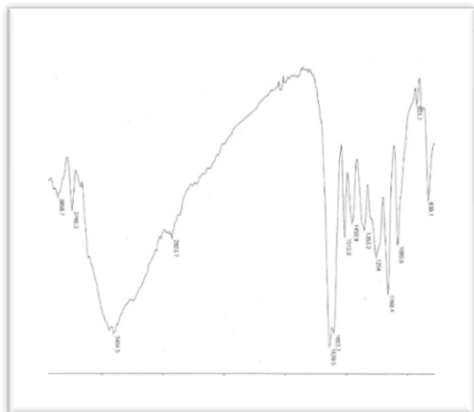


**Figure 4.** FT-IR Spectra of Spirulina

The spectrum in Figure 1 shows a broad absorption band at wavenumbers 3000–3600  $\text{cm}^{-1}$ , indicating absorption due to the O-H stretching vibration bonded to the central hydrogen at 3300  $\text{cm}^{-1}$ . The -OH group is part of the carboxylate group, which is enhanced by an absorption band at 1431  $\text{cm}^{-1}$ , representing the C-O stretching vibration. The N-H bending vibration of the amine group is recorded at a wavelength of 1596.0  $\text{cm}^{-1}$ . This group is part of the protein group, which is enhanced by an absorption band at 1637.0  $\text{cm}^{-1}$ , representing the C=O absorption (peptide bond). The siloxane component (Si-O-Si) is indicated by a sharp absorption band at 432.0  $\text{cm}^{-1}$ , indicating the Si-O-Si bending vibration, which is further enhanced by an absorption band at 363.0  $\text{cm}^{-1}$ , representing the C=O vibration. Si - O bend

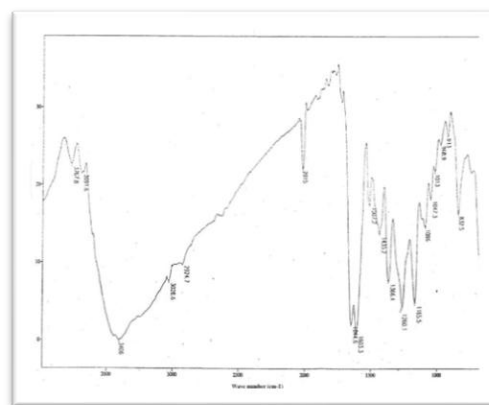


**Figure 5.** FT-IR Spectra of Immobilized Spirulina in Silicate

The spectral results show a wavenumber shift from 3364  $\text{cm}^{-1}$  to 3352  $\text{cm}^{-1}$ , indicating the presence of O-H stretching vibrations. The absorption at 759  $\text{cm}^{-1}$  represents the symmetric O-Si-O stretching (Tahir et al., 2026). The sharp absorption at 453  $\text{cm}^{-1}$  represents a wavenumber shift from 432  $\text{cm}^{-1}$ , indicating the Si-O-Si group. The absorption band at 800–1400  $\text{cm}^{-1}$  indicates the presence of C-O stretching vibrations of the carboxylate group, while the amine group shifts at 1629  $\text{cm}^{-1}$ . This is reinforced by the absorption band at 1089  $\text{cm}^{-1}$ , which is the amine group. The spectra in Figure 2 show the formation of new absorption bands. Therefore, the carboxylate and amine groups in the adsorbent plus are expected to play a better role in adsorbing Fe metal ions compared to the amine and carboxylate groups in unimmobilized *Spirulina* sp. biomass.

FTIR spectra of *Spirulina* showed characteristic bands at 3350–3364  $\text{cm}^{-1}$  (O–H/N–H stretching), 1630–1640  $\text{cm}^{-1}$  (amide I, C=O stretching), and 1400–1450  $\text{cm}^{-1}$  (carboxylate groups). After immobilization, new bands appeared at approximately 1089  $\text{cm}^{-1}$  and 453–759  $\text{cm}^{-1}$ , corresponding to asymmetric stretching and bending vibrations of Si–O–Si. The shift in O–H and amide bands suggests interactions between *Spirulina* functional groups and the silica network. These functional groups are expected to participate in  $\text{Fe}^{3+}$  adsorption through coordination and electrostatic interactions.

This study used FTIR as preliminary characterization to verify the presence of functional groups and silica network formation. Additional characterization using SEM-EDS, XRD, and BET surface area analysis is recommended in future work to provide more comprehensive evidence regarding morphology, elemental composition, crystallinity, and porosity.

### 3.6 Comparison of the Adsorption Capacity of BFA, Spirulina, and Immobilized Spirulina

One indicator of the effectiveness of adsorption of immobilized algae by Na-Silicate is to make a comparison of the adsorption capacity between every single adsorbent and compare it with the composite that has been prepared. The adsorption capacity of each adsorbent (BFA, Spirulina, and Na silicate-spirulina composite) was measured using UV-Vis Spectrophotometry at a maximum wavelength of 510 nm with time variations of 15 minutes, 30 minutes, 45 minutes, and 60 minutes for each adsorbent. Overall, the composite combining Spirulina and BFA demonstrated better adsorption performance compared to the other adsorbents in this study. The % Fe adsorbed data are as follows:

**Table 1.** Fe adsorption percentage for each adsorbent

No	Adsorbent	Time	Co mg/L	Ce mg/L	% adsorbed
1	BFA	15	125.235	118.65	5.26
2	Spirulina	15	125.235	110.85	11.49
3	Composite	15	125.235	105.65	15.64
4	BFA	30	125.235	100.25	19.95
5	Spirulina	30	125.235	99.78	20.33
6	Composite	30	125.235	99.86	20.26
7	BFA	45	125.235	98.65	21.23
8	Spirulina	45	125.235	88.85	29.05
9	Composite	45	125.235	80.89	35.41
10	BFA	60	125.235	78.85	37.04
11	Spirulina	60	125.235	68.98	44.92
12	Composite	60	125.235	60.65	51.57

The adsorption performance of bagasse fly ash (BFA), *Spirulina* biomass, and the BFA-*Spirulina* composite toward Fe<sup>3+</sup> ions was

evaluated at contact times of 15, 30, 45, and 60 min. The results are summarized in **Table 1** and demonstrate that the percentage of Fe<sup>3+</sup> removal increased with increasing contact time for all adsorbents. At the initial contact time of 15 min, the adsorption efficiencies were relatively low, with BFA removing only 5.26% of Fe<sup>3+</sup> whereas *Spirulina* and the composite removed 11.49% and 15.64%, respectively. The higher adsorption observed for *Spirulina* and the composite at this stage can be attributed to the abundance of readily accessible functional groups, such as hydroxyl, carboxyl, and amino groups, which rapidly interact with Fe<sup>3+</sup> ions through electrostatic attraction and complexation. At 30 min, all adsorbents exhibited a substantial increase in adsorption efficiency, reaching approximately 20%. Specifically, BFA, *Spirulina*, and the composite achieved Fe<sup>3+</sup> removal efficiencies of 19.95%, 20.33%, and 20.26%, respectively. This similarity suggests that during the early stages of adsorption, Fe<sup>3+</sup> uptake was primarily governed by external surface adsorption and rapid occupation of the most accessible active sites. More pronounced differences among the adsorbents became evident after 45 min of contact. At this time, BFA removed 21.23% of Fe<sup>3+</sup>, while *Spirulina* and the composite achieved 29.05% and 35.41%, respectively. The superior performance of the composite indicates that immobilization of *Spirulina* within the silica matrix enhanced the accessibility and stability of the biomass functional groups, while the porous structure of BFA facilitated diffusion of Fe<sup>3+</sup> ions to internal adsorption sites.

The improved adsorption capacity of the composite can be explained by the synergistic effect between the two components. BFA contributes a porous silica-rich support that enhances surface area and structural stability, whereas *Spirulina* provides abundant oxygen- and nitrogen-containing functional groups capable of binding Fe<sup>3+</sup>. In addition, immobilization prevents agglomeration of the algal particles and preserves the accessibility of adsorption sites, resulting in more effective metal uptake.

These findings were consistent with previous reports indicating that raw BFA exhibits relatively low adsorption performance due to limited active sites and low specific surface area, while modification or combination with biological materials significantly improves adsorption efficiency. The present results confirm that immobilization of *Spirulina* in a BFA-derived silica matrix is an effective strategy to enhance Fe<sup>3+</sup> removal from laboratory wastewater. Overall, the adsorption trend observed in this study can be summarized as follows:

### 3.7 BFA–Spirulina Composite > Spirulina > BFA

This order was maintained at all contact times and clearly demonstrates the advantage of combining mineral and biological components to produce a hybrid biosorbent with superior adsorption properties. Graphically, the data can be read in the following image on **Figure.6**

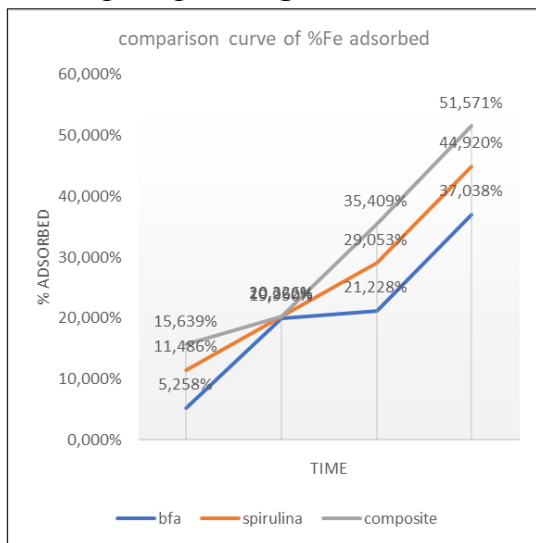


**Figure 6.** Performance Fe Percentage adsorption on each adsorbent

According to the study's findings, immobilized *Spirulina* plus BFA produced the maximum adsorption percentage, followed by *Spirulina* alone and BFA alone. *Spirulina*'s abundance of active groups that easily bind Fe<sup>3+</sup> is the reason for this. In essence, *spirulina* biomass is a "living organic material" that contains active chemical groups such as phosphate, sulfate,

hydroxyl (–OH), amino (–NH<sub>2</sub>), and carboxyl (–COOH) (Manfredi et al., 2025). These groups are all very good at binding metal ions. Because of interactions such as complex formation, coordination bonding, and electrostatic attraction, Fe<sup>3+</sup> ions easily attach to *spirulina*, making it similar to a chemical "stickysurface". *Spirulina*'s biological structure is susceptible to aggregate which means that its active surface isn't always completely open to bind Fe<sup>3+</sup>. In contrast, BFA offers a number of benefits, including a large surface area, numerous pores, and a small number of active groups. The residue from burning sugarcane bagasse is used to make BFA, or bagasse fly ash. With a huge surface area of hard, solid silica-alumina structure and numerous micro and mesopores, this material resembles a "mineral sponge" physically. Although BFA has few active groups and a weak interaction with multivalent metal ions like Fe<sup>3+</sup>, it is good at physically retaining particles or ions in its pores. As a result, it has a weaker adsorption capacity than *spirulina* (Yaseen et al., 2023).

When *Spirulina* is immobilized into BFA: Synergy Emerges. This is the key to why the BFA–*Spirulina* composite is the finest. Two potent characteristics come together when *Spirulina* is attached to the surface and pores of BFA: *Spirulina*'s active groups stay and are now more "exposed." Because it no longer clumps, *Spirulina* can maximize its active groups to capture Fe<sup>3+</sup>. In making this composite, the BFA structure makes *Spirulina* more stable. BFA acts like a scaffold that holds *Spirulina* in place, allowing Fe<sup>3+</sup> diffusion, preventing *Spirulina* from closing its own pores, and making it easier for Fe<sup>3+</sup> to find active sites. Fe<sup>3+</sup> ions are retained in the pores of BFA (physical adsorption), then encounter the active sites of *Spirulina* (chemical adsorption). These two mechanisms work in tandem, not interchangeably. It means all active surfaces are fully utilized.

#### 4. Conclusion

The result of this study shows that immobilizing *Spirulina* sp. biomass in a sodium silicate matrix effectively increases the adsorption capacity of Bagasse Fly Ash (BFA) toward  $Fe^{3+}$  ions in chemical laboratory wastewater. At 60 minutes of contact time, the BFA–*Spirulina* composite shows the best adsorption performance, with  $Fe^{3+}$  removal reaching 51.571%, outperforming both *Spirulina* alone (44.920%) and BFA alone (37.038%). A synergistic adsorption mechanism is responsible for the enhanced performance, wherein BFA's porosity structure facilitates physical adsorption, and *Spirulina*'s active functional groups facilitate chemical adsorption.

#### ACKNOWLEDGEMENT

The researchers would like to sincerely thank LPPM Universitas PGRI Madiun for providing the grant for this study.

#### REFERENCE

Ahmad, S., Wong, Y. C., & Veloo, K. V. (2018). Sugarcane bagasse powder as biosorbent for reactive red 120 removals from aqueous solution. *IOP Conference Series: Earth and Environmental Science*, 140(1). <https://doi.org/10.1088/1755-1315/140/1/012027>

Alnahhal, M. F., Hamdan, A., Hajimohammadi, A., Castel, A., & Kim, T. (2024). Hydrothermal synthesis of sodium silicate from rice husk ash: Effect of synthesis on silicate structure and transport properties of alkali-activated concrete. *Cement and Concrete Research*, 178(September 2023), 107461. <https://doi.org/10.1016/j.cemconres.2024.107461>

Apriyani, N. (2018). Industri Batik: Kandungan Limbah Cair dan Metode Pengolahannya. In *MITL Media Ilmiah Teknik Lingkungan* (Vol. 3, Issue 1).

Arita, S., Agustina, T. E., Ilmi, N., Dwi, V., & Pranajaya, W. (2022). *Treatment of*

*Laboratory Wastewater by Using Fenton Reagent and Combination of Coagulation-Adsorption as Pretreatment*. 23(8), 211–221.

Bhattacharjee, C., Dutta, S., & Saxena, V. K. (2020). A review on biosorptive removal of dyes and heavy metals from wastewater using watermelon rind as biosorbent. In *Environmental Advances* (Vol. 2). Elsevier Ltd. <https://doi.org/10.1016/j.envadv.2020.100007>

Collard, F. X., & Blin, J. (2014). A review on pyrolysis of biomass constituents: Mechanisms and composition of the products obtained from the conversion of cellulose, hemicelluloses and lignin. In *Renewable and Sustainable Energy Reviews* (Vol. 38, pp. 594–608). Elsevier Ltd. <https://doi.org/10.1016/j.rser.2014.06.013>

Fathurohman, M., Sukmawan, Y. P., Fauzi, M. R., & Tri, A. (2021). *Isolasi Biomaterial Silika dari Mikroalga Autotrofik dengan Variasi Air Laut Buatan*. 0(September), 201–208.

Fouad, M., Hamdan, A., Hajimohammadi, A., Castel, A., & Kim, T. (2024). Cement and Concrete Research Hydrothermal synthesis of sodium silicate from rice husk ash: Effect of synthesis on silicate structure and transport properties of alkali-activated concrete. *Cement and Concrete Research*, 178(September 2023), 107461. <https://doi.org/10.1016/j.cemconres.2024.107461>

Ichsan, A. S., Iswanto, N., Dewayanto, N., & Restu, O. (2025). *Life Cycle Assessment of Heavy Equipment Repair and Hazardous Waste Storage: Environmental Optimization at a Coal Mining Contractor*. 9(2), 69–90.

Kasman, M., Suzana, A., & Nur Hakim, A. (2022). ADSORPSI LIMBAH METHYLENE BLUE TERHADAP LIMBAH BIOMASSA NANAS Adsorpsi Limbah Methylene

- Blue terhadap Limbah Biomassa Nanas. *Jurnal Daur Lingkungan*, 5(1), 5. <https://doi.org/10.33087/daurling.v5i1.90>
- Leechart, P., Inthorn, D., & Thiravetyan, P. (2016). Adsorption of Antimony by Bagasse Fly Ash: Chemical Modification and Adsorption Mechanism. *Water Environment Research*, 88(9), 907–912. <https://doi.org/10.2175/106143015x14362865227030>
- Mall, I. D., Srivastava, V. C., & Agarwal, N. K. (2006). Removal of Orange-G and Methyl Violet dyes by adsorption onto bagasse fly ash - Kinetic study and equilibrium isotherm analyses. *Dyes and Pigments*, 69(3), 210–223. <https://doi.org/10.1016/j.dyepig.2005.03.013>
- Manfredi, C., Amoruso, A. J., Ciniglia, C., Giarra, A., Iovinella, M., Lombardo, F., Marano, A., Mondillo, N., Pinto, G., De Ballesteros, O. R., Trifuoggi, M., Vasca, E., & Balassone, G. (2025). Rare earth elements recovery from bauxite by biosorption onto *Galdieria sulphuraria*: A challenging case of study. *Journal of Environmental Chemical Engineering*, 13(5), 117781. <https://doi.org/10.1016/j.jece.2025.117781>
- Metwally, A. M., Aly, S. A. A., Makled, S. O., & Abdelkader, A. M. S. (2025). Biosorption of methylene blue from industrial wastewater using silicon dioxide nanoparticles and *Cladophora glomerata*. *Alexandria Engineering Journal*, 130(May), 115–138. <https://doi.org/10.1016/j.aej.2025.09.004>
- Mohamed, W. S. (2025). *Sustainable Water Treatment using SpiruSpheres: A Biosorbent Based on Spirulina platensis and Sodium Alginate*. 4338–4352.
- Morentera, B. G., Wahyuningsih, S., Hatining, D., & Sudarni, A. (2022). Pengaruh Variasi Waktu Kontak dan Dosis Adsorben Fly ash teraktivasi NaOH terhadap Adsorpsi Metilen Biru. *The Effect of Contact Time Variation and Dosage of NaOH-Activated Fly ash on Adsorption of Methylene Blue*. 19(3), 104–109.
- Moubayed, N. M. S., & Al-Houri, H. J. (2022). Characterization of adsorption ability of *Spirulina platensis* for copper ions removal from aqueous solutions. *Desalination and Water Treatment*, 250, 118–125. <https://doi.org/10.5004/dwt.2022.28111>
- Musnamar, A. A., Rahayu, A., Hakika, D. C., Zaini, N. A., Sari, H. P., Lestari, S. P., & Lim, L. W. (2025). Removal of Remazol Yellow from Textile Industry Wastewater by Quaternary Ammonium Polymer. 9(2), 100–107.
- Patel, H. (2020). a review †. 31611–31621. <https://doi.org/10.1039/d0ra06422j>
- Plana, P. D., Rodríguez, S. B., Villarejo, L. P., & Quesada, D. E. (2025). Synthesis of solid sodium silicate from waste glass and utilization on one - part alkali - activated materials based on spent oil filtering earth. *Environmental Science and Pollution Research*, 32(48), 27763–27785. <https://doi.org/10.1007/s11356-024-33368-w>
- Srivastava, V. C., Swamy, M. M., Mall, I. D., Prasad, B., & Mishra, I. M. (2006). Adsorptive removal of phenol by bagasse fly ash and activated carbon: Equilibrium, kinetics and thermodynamics. *Colloids and Surfaces A: Physicochemical and Engineering Aspects*, 272(1–2), 89–104. <https://doi.org/10.1016/j.colsurfa.2005.07.016>
- Subramanian, S., Pande, G., Weireld, G. De, & Giraudon, J. (2013). Sugarcane bagasse fly ash as an attractive agro-industry source for VOC removal on porous carbon. 49, 108–116. <https://doi.org/10.1016/j.indcrop.2013.04.014>
- Tahir, T., Druteikienė, R., Žukauskaitė, Z., Vaičiūnienė, J., Selskienė, A., Ignatjev, I., & Adnan, M. (2026). Biosorption of Lead (II) and cadmium (II) ions from aqueous solution by buckwheat

- (Fagopyrum Esculentum) hulls biosorbent: kinetic, equilibrium and thermodynamic studies. *Chemical Physics*, 602(September 2025). <https://doi.org/10.1016/j.chemphys.2025.112997>
- Warna, D. A. N., & Tekstil, L. (2016). *PENGGUNAAN BAGASSE FLY ASH UNTUK MEREDUKSI GAS H<sub>2</sub>S*. 411–414.
- Yaseen, N., Sahar, U., Bahrami, A., Mazhar Saleem, M., Ayyan Iqbal, M., & Saddique, I. (2023). Synergistic impacts of fly ash and sugarcane bagasse ash on performance of polyvinyl alcohol fiber-reinforced engineered cementitious composites. *Results in Materials*, 20(October), 100490. <https://doi.org/10.1016/j.rinma.2023.100490>
- Zhang, X., Li, H., Liu, L., Song, Y., Zhang, L., Miao, J., Jiang, J., Tian, H., Liu, C., Peng, F., & Tu, Y. (2025). Alginate lyase immobilized Chlamydomonas algae microrobots: minimally invasive therapy for biofilm penetration and eradication. *Acta Pharmaceutica Sinica B*, 15(6), 3259–3272. <https://doi.org/10.1016/j.apsb.2025.03.034>